THE JOURNAL OF COMPARATIVE NEUROLOGY 460:238–254 (2003)

Is There Remyelination during Aging of the Primate Central Nervous System?

ALAN PETERS* AND CLAIRE SETHARES
Department of Anatomy and Neurobiology, Boston University School of Medicine, Boston, Massachusetts 02118

ABSTRACT

The effect of aging on myelin sheaths in the rhesus monkey was studied in the vertical bundles of nerve fibers that traverse monkey cerebral cortex in primary visual area 17 and prefrontal area 46. As shown previously, with age the internodes of many of these myelin sheaths show structural changes, the most common of which is an accumulation of electron-dense cytoplasm within some sheaths, a change which is considered to indicate that breakdown of myelin is taking place. Supporting the suggestion that myelin is breaking down with age, astrocytes in the cortices of old monkeys contain phagocytosed myelin and some of the inclusion bodies in astrocytes label with antibodies to myelin basic protein. There is also evidence that remyelination is taking place. Thus, we have found an increase in the frequency of profiles of paranodes when transverse sections of the nerve fibers are examined. The increase in paranodal frequency with age is 57% in area 17 and 90% in area 46. This increase cannot all be attributed to lengthening of paranodes with age, because in area 17 the 11% increase in mean paranodal length with age is insufficient to account for an age-related increase in paranodal profile frequency. Consequently, there must be an increase in the number of internodal lengths of myelin with age, as would occur if shorter lengths of myelin are produced by remyelination. In support of the proposal that remyelination is occurring, short internodal lengths of myelin have been found in the nerve bundles passing through the cortices of old monkeys and inappropriately thin sheaths occur around some axons. Both of these features are generally considered to be the hallmarks of remyelination. Consequently, it is proposed that in the aging cerebral cortex of the monkey there is some breakdown of internodes of myelin with subsequent remyelination that leads to the formation of some new and shorter internodal lengths of myelin. J. Comp. Neurol. 460:238–254, 2003.

Indexing terms: normal aging; nerve fibers; myelin; paranodes; rhesus monkey; cerebral cortex; cognition

In earlier studies we have shown that as a consequence of aging there are alterations in the structure of some internodes of myelin sheaths in the central nervous system of nonhuman primates (Feldman and Peters, 1998; Peters, et al., 2000; Peters and Sethares, 2002). The age-related structural alterations are basically of four types. The most common alteration is a localized splitting of myelin sheaths at the major dense line to form pockets containing electron-dense cytoplasm. Because of its location, the dense cytoplasm must belong to the oligodendrocyte forming the sheath. In other cases the intraperiod line is split and sheaths balloon out to form blebs that appear to be fluid-filled. Some ballooned sheaths may have dense cytoplasm at their bases and the balloons are of various sizes, with some being as large as 10 μm in diameter. Third, thick myelin sheaths can show circumferential splitting, giving the impression that there is a "double" sheath consisting of one set of compact lamellae surrounded by a second set. And finally, with increasing age redundant sheaths (Sturrock, 1976) become more common. In profiles of redundant sheaths the axon is seen

Grant sponsor: National Institute of Health/National Institute on Aging; Grant number: 1PO AG 00001.

*Correspondence to: Alan Peters, Department of Anatomy and Neurobiology, Boston University School of Medicine, 715 Albany Street, Boston, MA 02118. E-mail: apeters@cajal-1.bu.edu

Received 14 November 2002; Revised 7 January 2003; Accepted 10 January 2003

DOI 10.1002/cne.10639

Published online the week of April 7, 2003 in Wiley InterScience (www.interscience.wiley.com).

TABLE 1. Percentage of Profiles of Paranodes and Nodes in Area 17 and Area 46

AM number	Age	Sex	Area 17		Altered internodes	Area 46		Altered internodes	CII
			Paranodes	Nodes		Paranodes	Nodes		
AM 58	4yrs	M	7.3%	1.0%	1.3%	Not available	Not available		No data
AM 16	5yrs	M	7.6%	1.7%	0.8%	6.1%	1.1%	1.3%	0
AM 76	6yrs	F	9.6%	0.8%	0.5%	6.0%	1.3%	0.3%	0.09
AM 77	6yrs	F	6.4%	1.0%	0.9%	6.1%	0.6%	0.9%	1.14
AM 47	9yrs	M	10.9%	1.0%	0.6%	5.3%	0.5%	1.0%	−0.54
AM 96	9yrs	F	8.7%	2.0%	1.5%	8.8%	1.3%	1.3%	2.46
AM 53	10yrs	M	7.0%	2.1%	0.7%	6.0%	1.3%	1.8%	0.08
		Means	8.2 ± 1.6%	1.4 ± 0.5%		6.4 ± 1.2%	1.0 ± 0.4%		
AM 19	25yrs	F	16.5%	2.1%	2.5%	12.9%	1.5%	4.0%	1.68
AM 100	25yrs	F	11.2%	1.1%	5.6%	9.5%	1.0%	5.2%	4.12
AM 12	27yrs	F	12.7%	2.3%	5.5%	11.9%	2.6%	4.8%	4.05
AM 15	27yrs	F	11.5%	1.6%	4.8%	10.2%	2.5%	5.7%	1.56
AM 62	27yrs	M	13.5%	1.3%	5.4%	13.8%	3.2%	5.2%	4.26
AM 27	27yrs	M	11.0%	1.2%	6.3%	10.4%	1.1%	4.0%	1.34
AM 26	29yrs(est)	F	12.9%	2.2%	2.3%	9.7%	1.2%	4.0%	0.94
AM 17	29yrs(est)	F	11.0%	1.7%	8.3%	13.8%	1.7%	8.4%	3.24
AM91	32yrs	M	13.9%	1.4%	4.3%	14.6%	2.1%	2.8%	0.17
AM 41	32yrs	F	11.5%	1.5%	7.3%	12.0%	1.1%	6.2%	4.81
AM 13	35yrs(est)	M	16.5%	2.1%	4.8%	15.6%	3.4%	6.3%	No data
		Means	12.9 ± 2.0%	1.7 ± 0.4%		12.2 ± 2.1%	2.0 ± 0.9%		

to be located at one side of a myelin sheath that is many sizes too large for the enclosed axon. In both area 17 and in area 46, the frequency of these structural changes in myelin correlate with both increasing age and with reduced cognitive abilities of the monkeys (Peters et al., 2000; Peters and Sethares, 2002).

Both the accumulation of dense cytoplasm within myelin sheaths and the formation of balloons are probably degenerative changes, while the age-related increases in the frequencies of redundant myelin and of thick sheaths appear to be related to the continued production of myelin lamellae (Peters et al., 2001b). Thus, when the myelin sheaths in the vertical bundles of nerve fibers in primary visual cortex of young monkeys (4–9 years of age) are compared with those from old monkeys (over 24 years of age), it is found that sheaths in old monkeys are thicker than those in young monkeys: the mean number of myelin lamellae in the sheaths of young monkeys is 5.6, while in old monkeys the mean number is 7.0. Much of this increase in mean thickness occurs because myelin sheaths with more than 10 lamellae become increasingly common in older monkeys, and it these sheaths that frequently split to produce the appearance of "double" sheaths (Peters et al., 2001b). The conclusion from these studies is that while there is some degeneration of myelin with age, there is a concomitant continued production of myelin lamellae.

In other studies we have shown that with age there appears to be an increase in the numbers of oligodendrocytes in monkey primary visual cortex (Peters et al., 1991a) and that groups and rows of oligodendrocytes become increasingly common (Peters, 1996). These observations suggest that oligodendrocytes proliferate during aging and this raises the question of why additional oligodendrocytes are required. One reason could be to remyelinate axons whose sheaths have degenerated. The possibility that remyelination might be taking place during aging was reinforced during an examination of profiles of cross-sectioned myelin sheaths in the vertical bundles of nerve fibers in primary visual cortex (Peters et al., 2001b). It was noticed that there is an increase in the frequency of profiles of paranodes in older monkeys. This could be taken to indicate that with age there is an increase in the number of internodal lengths of myelin. Such a change would take place if some internodes of myelin had degenerated and been replaced with new and shorter lengths of myelin, as occurs in remyelination (e.g., Prineas and McDonald, 1997).

The present article investigates the question of whether there is degeneration of myelin followed by remyelination in the cortices of old monkeys. The data to be presented quantify the age-related increases in the frequency of profiles of paranodes in cross-sections of the vertical nerve fiber bundles present in both primary visual cortex and in prefrontal area 46. It will be argued that this data, as well as the presence of phagocytosed myelin in astrocytes, the existence of short internodal lengths of myelin, and of some inappropriately thin myelin sheaths in the cortices of old monkeys, support the concept that during aging some myelin internodes degenerate and are replaced by new and shorter ones.

MATERIALS AND METHODS

Animals

Eighteen rhesus monkeys (*Macaca mulatta*) were used in this study. Seven of the monkeys were young (4–10 years of age) and 11 of them were old monkeys (over 25 years of age). The ages of the monkeys, given to the nearest whole year, and their sexes are given in Table 1. For three of the older monkeys that were not born in captivity the ages have had to be estimated (est). Details of the protocol for fixing the brains of these monkeys are given in an earlier publication (Peters et al., 1994). The perfusions were carried out in full accordance with the approved Institutional Animal Care and Use Committee regulations. In summary, the monkeys were preanesthetized with ketamine (6.5 mg/kg). Sodium pentobarbital was then administered intravenously (~35–45 mg/kg) until a monkey was deeply anesthetized and a state of areflexia was achieved. The monkeys were then intubated into the trachea and artificially respired with a mixture of CO_2 and O_2. The chest was opened and the monkeys perfused intracardially with a warm solution of 1% paraformaldehyde and 1.25% glutaraldehyde in 0.1 M cacodylate or phosphate buffer at pH 7.4. Following this initial perfusion, the brain was removed and one hemisphere fixed for several

more days in a cold solution of 2% paraformaldehyde and 2.5% glutaraldehyde in a 0.1 M buffer of the same type as used for the perfusion.

Tissue preparation

Several tissue blocks, ~2 mm thick, were taken both from area 46 of prefrontal cortex and from the primary visual cortex, area 17, of each monkey. The blocks of primary visual cortex were taken from the opercular surface of the occipital lobe, about 3 mm caudal to the lunate sulcus, where the center of the visual field is represented. The blocks of area 46 were taken from the floor of the principal sulcus at the level of the rostral end of the corpus callosum (see Peters et al., 1994). This portion of prefrontal cortex is part of area 8 of Brodmann (1905) and is designated by Walker (1940) as belonging to area 46. All blocks of cerebral cortex were osmicated, dehydrated in an ascending series of alcohols, then embedded in Araldite.

The blocks of cortex were first sectioned vertically, that is, at right angles to the pial surface, and semithick sections stained with Toluidine blue to determine the location of layer 4. In addition, thin sections were cut in the vertical plane to examine internodal lengths of myelin and to obtain micrographs from which the lengths of paranodes in the nerve fibers contained in the vertical bundles could be measured. The tissue blocks were then turned to obtain sections passing horizontally through layer 4. After a series of semithick sections had been prepared for light microscopy, thin sections were taken for electron microscopy.

For visual cortex the horizontal sections were taken at the level of layer 4Cβ, where the vertically oriented fibers consistently aggregate into discrete and compact bundles (Peters and Sethares, 1996; Nielsen and Peters, 2000). In area 46, layer 4 is of variable thickness and the bundles of myelinated nerve fibers often vary in size. In addition, their constituent nerve fibers are less compact than in area 17 and many horizontally oriented fibers pass through the bundles. These factors sometimes make it difficult to be certain that a section is passing exactly through layer 4, and so some sections also contained portions of the adjacent lower layer 3 or upper layer 5 (Peters and Sethares, 2002).

All of the thin sections were stained with uranyl acetate and lead citrate for examination in a JEOL 100S electron microscope.

Quantitative analysis of profiles of nerve fibers

After the thin sections through layer 4 of areas 17 and 46 had been examined to determine the quality of fixation and the effects of age on the morphology of the nerve fibers, electron micrographs were taken at magnifications of between ×4,000 and ×10,000 and printed at an enlargement of ×2.5. For each monkey the profiles of at least 500 transversely sectioned fibers in the bundles were examined and a determination made of the percentage of those profiles that belonged to nodes of Ranvier, to paranodes, or to internodes.

In addition to a determination of the frequency of profiles of internodes, paranodes, and nodes, the frequency of internodal profiles of sheaths with altered myelin was assessed. With the exception of AM 77, AM 96, and AM 13, data on the frequency of profiles of internodes with altered sheaths in area 17 was available as previously published (Peters et al., 2000), as had data for the frequency of altered internodal sheaths in area 46 (Peters and Sethares, 2002).

Lengths of paranodes

To determine if age has any effect on the lengths of paranodes, vertically oriented thin sections through the bundles of nerve fibers in area 17 of three young (AM 16, AM 76, and AM 77) and three old (AM 12, AM 15, and AM 26) monkeys were examined. Electron micrographs were taken only of profiles of longitudinally oriented nerve fibers that displayed at least one complete paranode, with a sufficient length of the adjacent compact myelin to count the number of lamellae in the internodal sheath. The number of lamellae in the internodal sheaths was counted directly from the image screen of the electron microscope. Micrographs of the paranodes were then taken at a primary magnification of ×8,000 and the lengths of the paranodes measured directly from the electron microscopic negatives.

Antibody labeling of neuroglial cell inclusions

The purpose of this part of the study was to determine if myelin is phagocytosed by neuroglial cells, and because myelin basic protein (MBP) is one of the most common constituents of myelin, it was decided to determine if antibodies to MBP bind to inclusions in neuroglial cells. However, the binding sites of the MBP antibody could not be assessed using the DAB reaction because the inherent density of many of the inclusions in astrocytes, microglial cells, oligodendrocytes, and pericytes are of the same electron density as the DAB reaction product. Consequently, an immunogold, silver amplification procedure was used.

Sections were labeled with an antibody to myelin basic protein (Sternberger Immunochemicals, Lutherville, MD cat# SMI 99) and the binding sites visualized using an immunogold silver amplification system (Auroprobe™ One, cat# RPN-471 and IntenSE™M, cat# RPN-491, Amersham, Arlington Heights, IL). The protocol used for the procedure was modified from the product protocol supplied by Amersham.

Fifty-μm thick, vibratomed sections from area 17 of monkey AM 100 (25 years old) were pretreated with 1% sodium borohydride for 30 minutes, rinsed, and preincubated in a mixture of 1% normal goat serum, 0.8% bovine serum albumin (BSA), 0.1% sodium azide, 0.1% Triton-X, and 0.1% gelatin solution (supplied with the Auroprobe™ One kit) in 0.1 M PBS for 1 hour, then transferred to a solution containing the antibody to myelin basic protein, diluted to 1:100. After incubation overnight in the primary antibody solution, sections were rinsed in a solution containing 0.8% BSA, 0.1% sodium azide, and 0.1% gelatin in 0.1% PBS. They were then incubated in 1 nm gold-labeled goat antimouse IgG (Auroprobe™ One, Amersham) for 3 hours. After rinsing, the sections were treated with the silver enhancement solution (IntenSE™M, Amersham) and monitored by light microscopy, until the binding sites of the primary antibody were revealed. The sections were then embedded in Araldite resin, sectioned at 50–70 nm on an ultramicrotome, mounted on grids, stained with uranyl acetate and lead citrate, and viewed in the electron microscope.

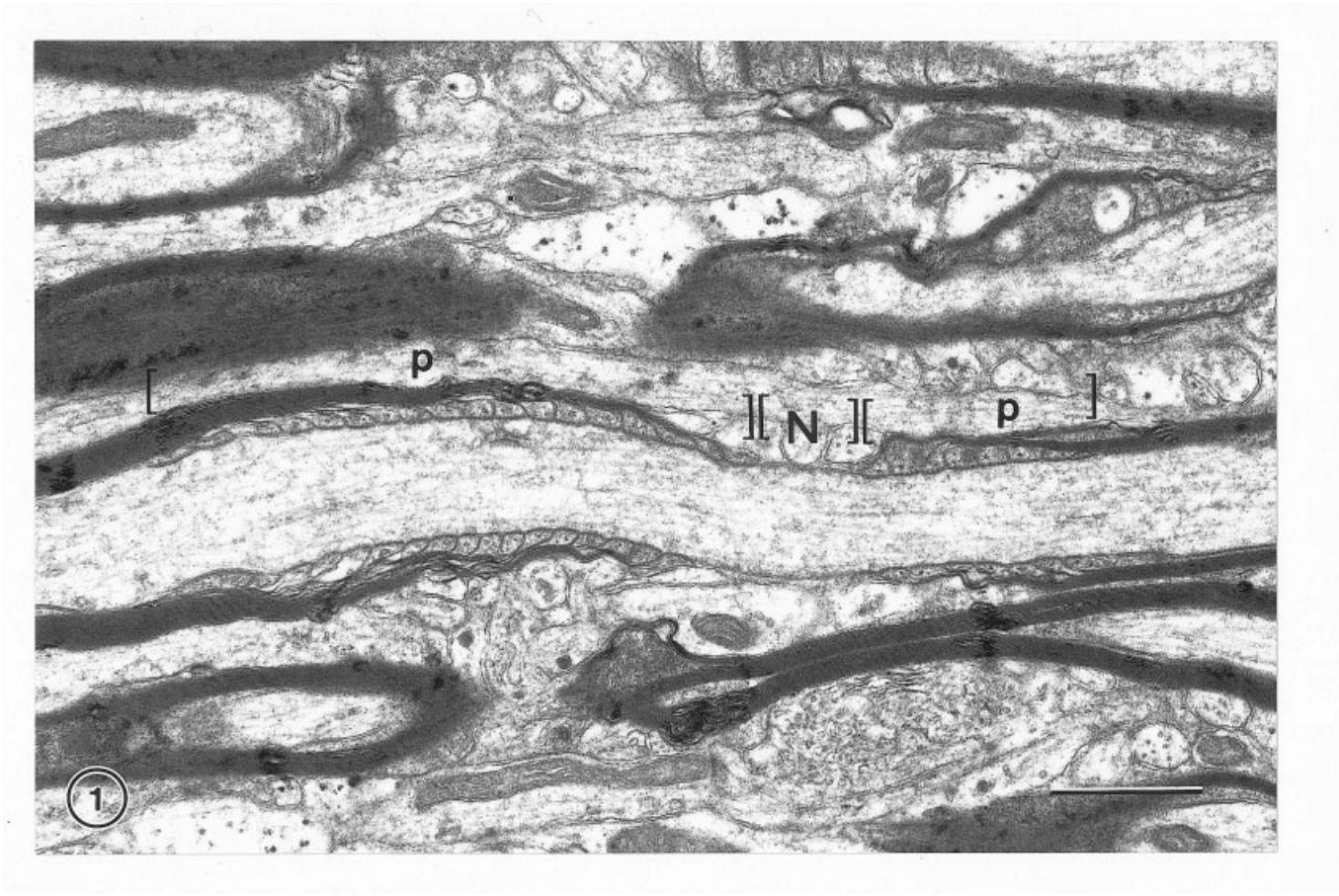

Fig. 1. Longitudinal section of a nerve fiber in one of the vertical bundles from area 17 of a 32-year-old monkey, AM 41. The section passes through a node of Ranvier (N), where the axolemma is characterized by the presence of a dense undercoating. On each side of the node are the paranodes (p). Note that the sheaths on each side of the node are of different thicknesses. The sheath on the right side has 8 lamellae, while the one of the left has 15 lamellae and consequently has a longer paranode. Scale bar = 1 μm.

As controls, other sections were processed using the same procedure as described above, but omitting the primary antibody. No background labeling was detected.

Behavioral testing

All monkeys were administered a battery of behavioral tasks to assess learning and memory. The battery of tests included three visual recognition memory tasks: the delayed nonmatching to sample (DNMS) task, a DNMS task with a 2-minute delay, and the delayed recognition memory span (DRST) task. Details of how these tasks were performed are given in earlier publications (e.g., Herndon et al., 1997; Killiany et al., 2000; Peters et al., 2000).

Although it is important to identify deficits in individual cognitive domains, we have found it useful to formulate a measure of overall cognitive impairment (Herndon et al., 1997; Peters et al., 1998) and this is the Cognitive Impairment Index (CII), which is derived from the normalized scores achieved by a monkey on each of the three behavioral outcome measures used in the battery of tests. In effect, the mean CII for young monkeys is 0 and the higher the CII value the more a monkey is impaired. The CIIs for the monkeys used in this study are given in Table 1, although no data were available for two monkeys, AM 13 and AM 58.

RESULTS

Internodes, paranodes, and nodes

The sheaths of myelinated nerve fibers are formed by oligodendrocytes and the sheaths consist of lengths of myelin separated by nodes of Ranvier. As a length of myelin approaches a node the lamellae of the sheath begin to terminate at a paranode (Fig. 1; p). In longitudinal sections through paranodes (Fig. 1), the innermost lamella can be seen to end first and successive turns in the spiral of myelin lamellae terminate progressively, each turn overlapping the one beneath. Thus, the sheath gradually becomes thinner and the outermost lamella terminates closest to the node of Ranvier (Fig. 1; N). As the lamellae terminate in this fashion, the major dense line of the sheath opens up to accommodate cytoplasm, and because of the gradual way in which the lamellae terminate, this cytoplasm is contained in a helical tunnel. In longitudinal sections through a paranode, profiles of this helix appear

as a series of cytoplasm-containing loops on each side of the enclosed axon. The termination of the myelin leaves the axolemma essentially bare at the node of Ranvier, although in some large axons the node appears to be partially covered by astrocytic processes.

For present purposes, each length of myelin can be considered to consist of two separate domains: the internodal myelin sheath in which the myelin is compact, and the paranodes where the lamellae terminate. For more detailed descriptions of the structure of myelinated nerve fibers in the CNS, reference can be made to accounts such as those given by Raine (1984), Peters et al. (1991b), and Rosenbluth (1995).

In transversely sectioned myelinated nerve fibers, profiles of the internodal myelin domain (Fig. 2; i) are recognized by the fact that the myelin of the sheath is compact and the plasma membrane on the inside of the sheath is separated from the axolemma by a space (Peters et al., 1991b). In contrast, in profiles of transversely sectioned paranodes the axolemma and the plasma membrane on the inside of the sheath come together to form a complex junction in which these two trilaminar membranes are closely apposed and separated by a gap of only 3 nm (Figs. 2–4). Consequently, at high magnification the junction appears as four dark layers separated by three alternating pale zones (Fig. 3). Moreover, in cross-sectional profiles of paranodes, the outline of the axon, and hence of the junctional complex, is very regular and the cytoplasm in the helical tunnel usually appears as a complete ring of cytoplasm separating the junctional complex from the inside of the compact myelin. Of course, the number of compact lamellae present in sections through paranodes depends on the proximity to the node (see Fig. 2). In longitudinal sections through paranodes, a much more complex intermembranous structure is apparent, for the paranodal loops of cytoplasm indent the surface of the axon (Fig. 1) and at higher magnifications the junction between the axolemma and the inner membrane of the myelin sheath shows regularly spaced densities of transverse bands (e.g., see Peters, 1966; Bhat et al., 2001). However, these features are not seen in transverse sections of paranodes.

At the node of Ranvier the axon is devoid of a sheath, but sections through the nodal axon can be recognized because of the distinctive undercoating on the cytoplasmic face of the axolemma (Fig. 4). It is now known that much of this coating is due to the presence of complexes of cytoskeletal molecules and ankyrin, which are necessary for the concentration of sodium channels in this region (e.g., Bennett and Lambert, 1999). In addition, the cytoplasm of the nodal axon usually contains a higher concentration of microtubules than other parts of the axon. It might be mentioned that some cross-sectioned initial axon segments can also appear in the thin sections. At the axon initial segment there is also an undercoating of the axolemma, but axon initial segments can be recognized because most of the microtubules in the axoplasm are in fascicles (see Peters et al., 1991b).

Frequency of paranodes and nodes in the myelin bundles of areas 17 and 46

As described in previous articles (Peters and Sethares, 1996; 2000, 2001b), at the level of layer 4Cβ horizontal sections of primary visual cortex show the vertically oriented myelinated nerve fibers to be organized into compact bundles (Fig. 5). In contrast, at the level of layer 4 in area 46 of prefrontal cortex, the vertical bundles of myelinated nerve fibers are more loosely defined, because the constituent nerve fibers are spaced further apart (Fig. 6). Moreover, in area 46 numerous horizontal nerve fibers criss-cross through the bundles (Peters and Sethares, 2002). In addition to the myelinated nerve fibers, in both areas 17 and 46 the bundles contain unmyelinated nerve fibers, as well as some dendrites and processes of astrocytes and oligodendrocytes.

In young monkeys transverse sections of the nerve fibers in the vertical bundles have sheaths in which the myelin is generally compact, although there may be a local shearing of the lamellae in one segment of the profiles of some sheaths. This type of localized shearing, in which the lamellae are split apart and become detached from one another, is considered to be due to poor fixation. It is quite different from that which occurs at Schmidt-Lanterman incisures, where the major dense line opens up to produce funnel-like clefts containing cytoplasm (see Peters et al., 1991b). However, in older monkeys (over 25 years of age), and to a much lesser extent in young monkeys (4 to 10 years of age), there are additional alterations in the morphology of myelin sheaths. These alterations, which are age-related, have been described in detail elsewhere (Feldman and Peters, 1998; Peters et al., 2000; Peters and Sethares, 2002). To briefly reiterate, the alterations are of the following types. The most common alteration is one in which the major dense line of myelin sheath is split to enclose electron-dense cytoplasm (see Figs. 5, 6). Less commonly, the intraperiod line becomes split and contains fluid, so that the sheath balloons out to one side (Fig. 5). Also, with age the number of nerve fibers with thicker myelin sheaths increases (Peters et al., 2001b) and such thick sheaths may become circumferentially split (Fig. 5), sometimes giving rise to the appearance of a double sheath. Yet other nerve fibers have redundant myelin, so that the sheath is too large for the size of the enclosed axon. The frequency with which profiles of internodal portions of myelin sheaths in areas 17 and 46 of individual monkeys show sheaths with these age-related alterations is given in Table 1. It will be seen that, in general, there is an increase in the frequency of altered internodal profiles with age.

Electron micrographs of cross-sections of myelinated nerve fibers in the vertical bundles in area 17 and in area

Fig. 2. Transversely sectioned nerve fibers from area 46 of a 25-year-old monkey, AM 100. One of the nerve fibers (i) is sectioned through an internode. Two others, p_1 and p_2, are sectioned through paranodes, as shown by the junction formed between the axolemma and the membrane on the inside of the sheath. p_2 is much closer to the node than p_1. Scale bar = 0.5 μm.

Fig. 3. Transversely sectioned paranode from area 46 of a 25-year-old monkey, AM 100, to show the seven-layered junction (arrowheads) between the axolemma and the membrane on the inside of the sheath. Scale bar = 0.2 μm.

Fig. 4. Transversely sectioned nerve fibers from a 27-year-old monkey, AM 27. One nerve fiber (p) is sectioned at the level of the paranode and shows the ring of cytoplasm (asterisk) in the helical tunnel. Another nerve fiber (N) is sectioned through the node of Ranvier, as indicated by the dense undercoating of the axolemma (arrow). Scale bar = 0.5 μm.

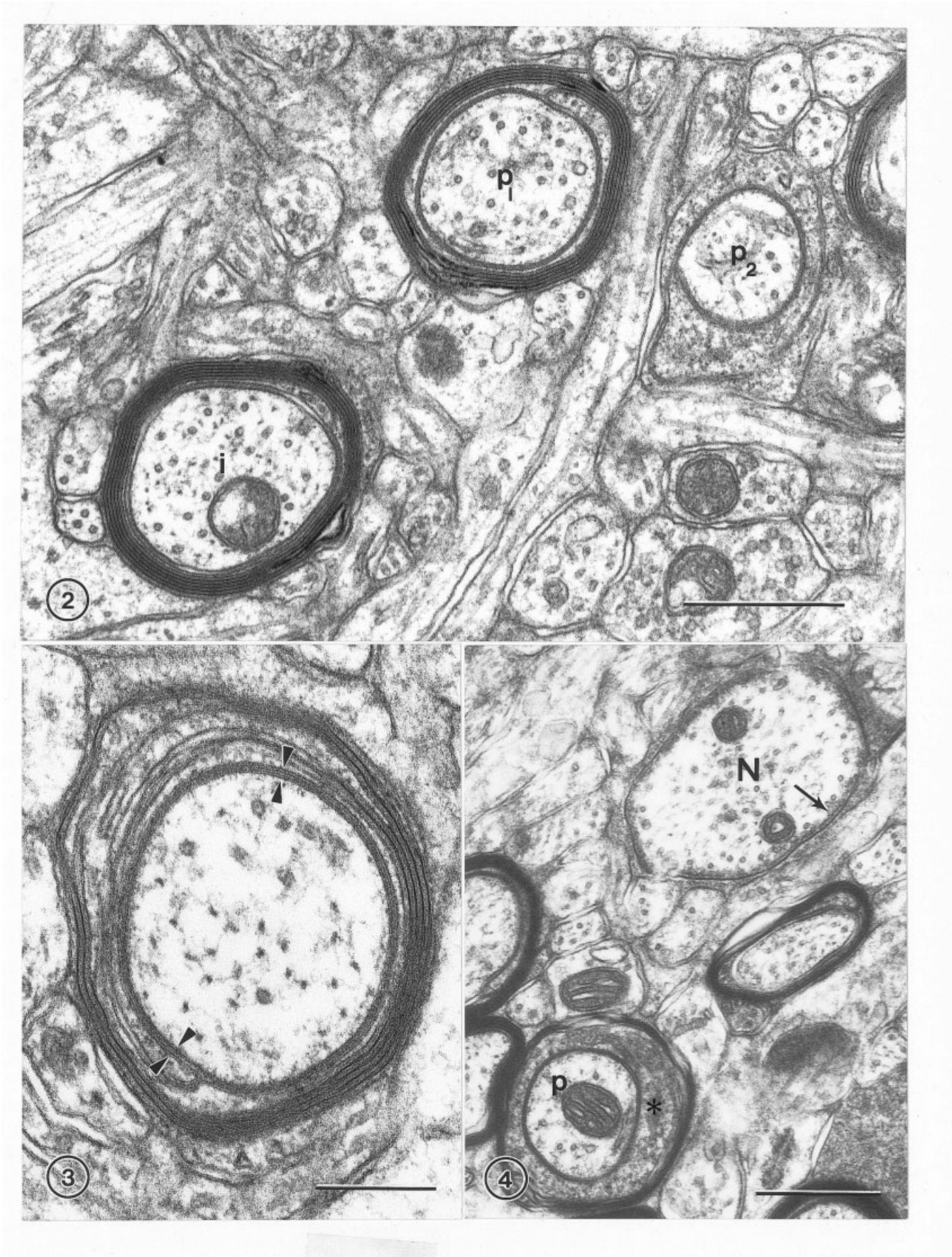

Figures 2–4

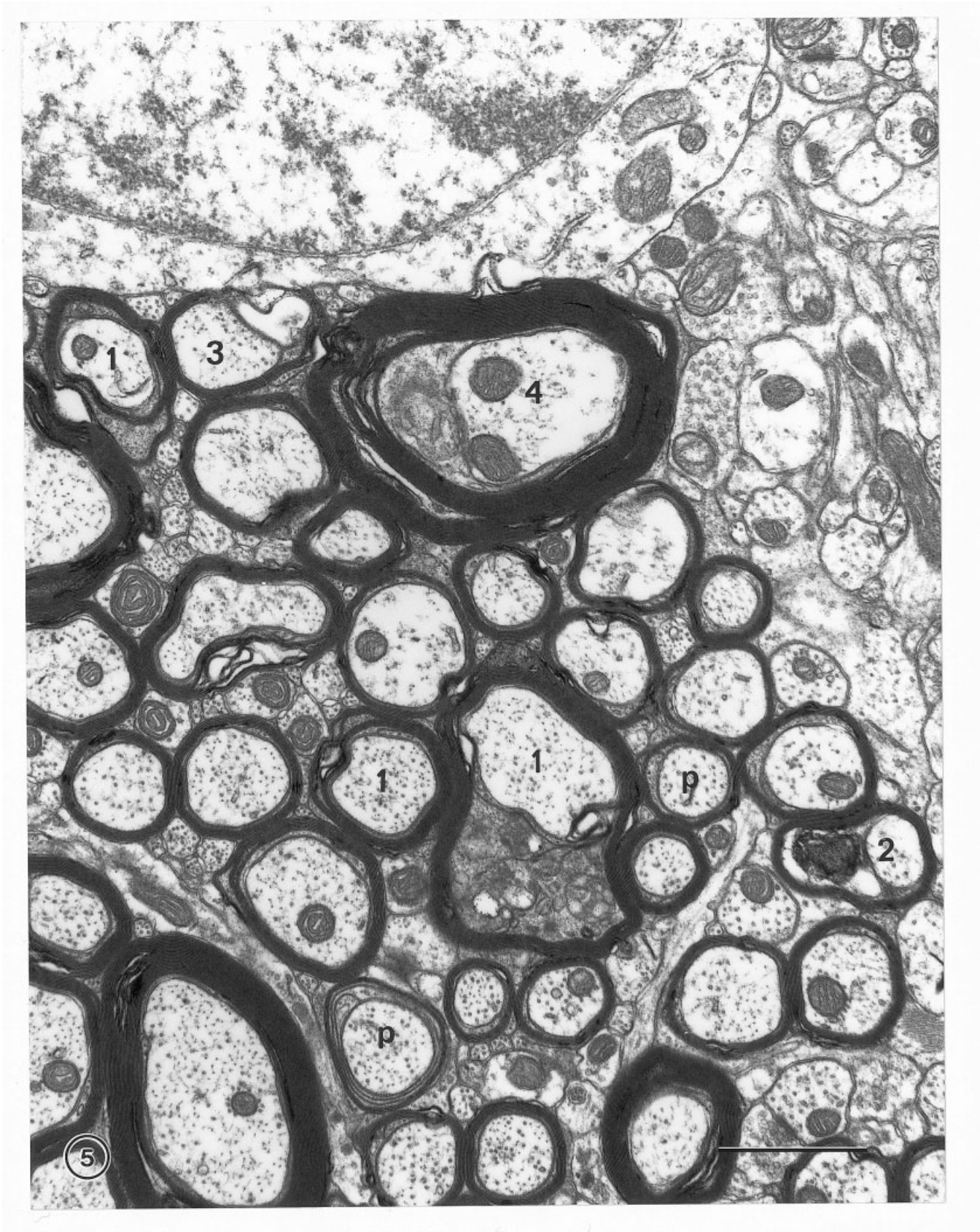

Fig. 5. Transversely sectioned bundle of myelinated nerve fibers from layer 4C of area 17 in a 29-year-old monkey, AM 17. Three of the nerve fibers (1) in the bundle show splitting of their sheaths to accommodate dark cytoplasm. Another nerve fiber (2) has a dense inclusion in the cytoplasm inside its sheath, while another (3) has a fluid-containing blister. Also note the splitting of the thick sheath surrounding the large axon (4). This field contains profiles of two paranodes (p). Scale bar = 1 μm.

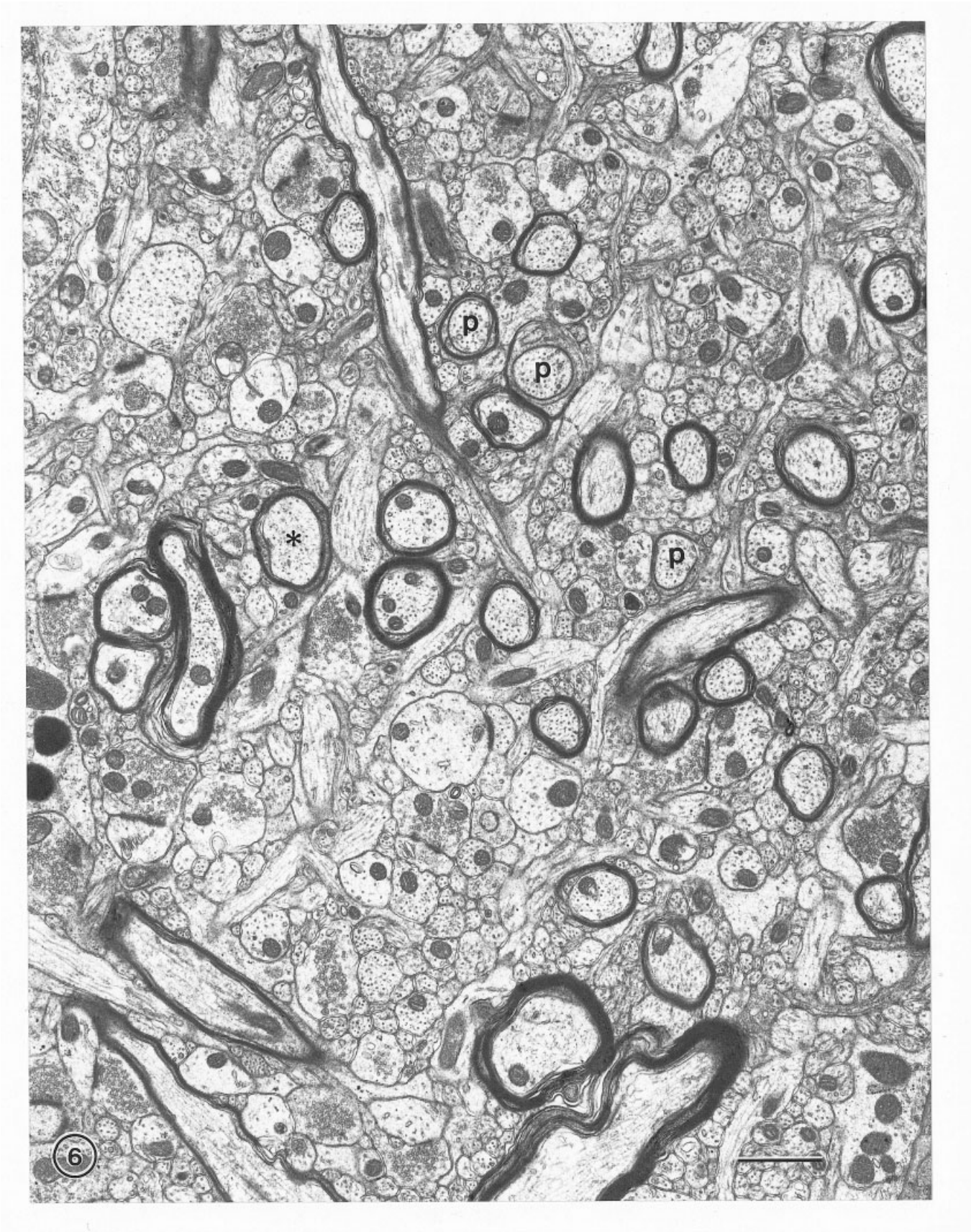

Fig. 6. A bundle of myelinated nerve fibers from area 46 of a 25-year-old monkey, AM 100. The nerve fibers of the bundles in area 46 are more loosely packed than those in area 17. Three of the nerve fibers (p) have been sectioned through paranodes, as evidenced by the thinness of the sheaths and by presence of a junction between the axolemma and the plasma membrane on the inside of the myelin sheath. The remainder are sectioned through internodes, and one of them (asterisk) shows a splitting of the sheath to accommodate dense cytoplasm. Scale bar = 1 μm.

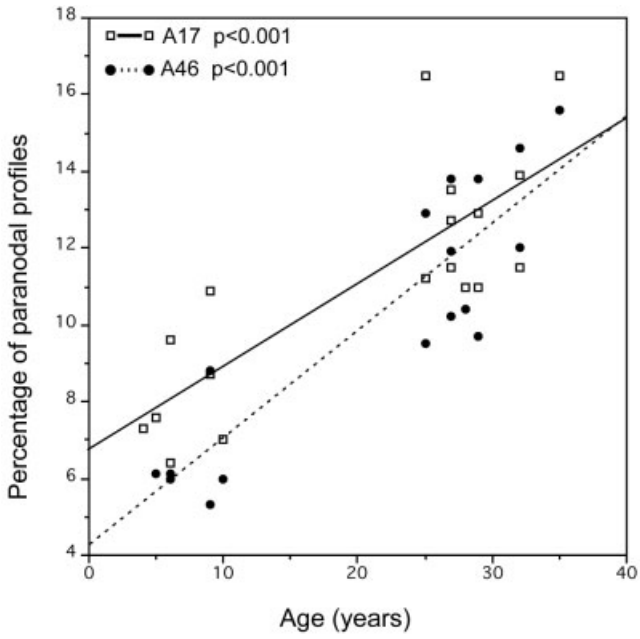

Fig. 7. A plot of the percentage of nerve fiber profiles of paranodes vs. age in both area 17 and area 46.

46 were examined to determine if there is a change with age in the frequency of profiles of internodes, paranodes, and nodes of Ranvier. Profiles of these three domains were identified on the basis of the criteria given above. It needs to be pointed out that although profiles of internodes and paranodes can be readily recognized, it is more difficult to be certain that all profiles of nodes of Ranvier have been recognized. Identification of profiles of nodes basically relies on the presence of the undercoating of the axolemma (see Fig. 4), and if the undercoating is not well developed it can be difficult to distinguish between the profile of a node of a small nerve fiber and the profile of one of the larger unmyelinated nerve fibers contained in a nerve bundle.

The results of the profile analysis are given in Table 1, in which it will be seen that in primary visual cortex of young monkeys a mean of 8.2 $\pm$ 1.6% of the profiles of myelinated nerve fibers belong to paranodes, while in the old monkeys the frequency of paranodal profiles is increased to a mean of 12.9 $\pm$ 2.0%. Consequently, in area 17 there is a 57% increase in the frequency of paranodal profiles with age. In area 46 of prefrontal cortex the comparable values are that 6.4 $\pm$ 1.2% of the profiles belong to paranodes in young monkeys, with an increase to a mean of 12.2 $\pm$ 2.1% of profiles in the old monkeys, giving a 90% increase in paranodal profiles with age. As can be seen in Fig. 7, in both area 17 and in area 46 there is a significant correlation ($P < 0.001$) between age and the increase in frequency of profiles of paranodes.

As far as nodes of Ranvier are concerned, the data in Table 1 show that while there is a trend towards an increase in the number of their profiles when young and old monkeys are compared, the difference is not significant. This may be partly due to the difficulty in recognizing all profiles of nodes of Ranvier.

Correlation between the frequency of paranodes and of altered sheaths

The data in Table 1 show that with age there is a significant increase in the frequency of altered internodal sheath profiles in both area 17 (also see Peters et al., 2000) and area 46 (also see Peters and Sethares, 2002). Since there is also an increase in the frequency of paranodal profiles with age (Fig. 7), the consequence is that in the population of monkeys examined there is a good correlation between the increased frequency of occurrence of altered sheaths and the increased frequency of occurrence of paranodes ($P < 0.05$).

Lengths of paranodes

The 59% increase in the frequency of paranodal profiles in area 17 of the older monkeys and the 90% increase in area 46 could be due to several factors. One factor that needs to be considered is the possibility that there is an inherent increase in the lengths of paranodes with age, such that in sheaths of the same thickness the paranodes are appreciably longer in old monkeys. To examine this possibility, vertically oriented thin sections were taken through the primary visual cortex of three young (AM 16, AM 76, and AM77) and three old (AM 12, AM 15, and AM26) monkeys, so that longitudinal sections of nerve fibers could be examined. Electron micrographs were taken of a total of 96 paranodes in the group of young monkeys and 90 paranodes in the group of old monkeys. For each example the number of lamellae in the adjacent internode was counted directly from the viewing screen of the electron microscope and then the paranode photographed at $\times$8,000. The length of a paranode was measured directly from the photographic negative. A paranode is defined by the presence of cytoplasm-containing loops and was taken to extend from where the sheath terminates adjacent to the node of Ranvier to where the innermost lamella of myelin opens up to enclose the first loop of cytoplasm (see Fig. 1). The extent of a paranode also usually coincides with the extent of the regularly spaced densities of the transverse bands.

The results of this analysis are given in Figure 8, in which the numbers of lamellae in the sheaths are plotted against the lengths of the paranodes. It will be seen that, except for the 15% of nerve fibers with more than 10 lamellae in the old monkeys (Peters et al., 2001b), there is only a small, although significant, difference in the lengths of paranodes when sheaths of the same thickness are compared in young and old monkeys. However, the increase in the mean thickness of myelin sheaths with age needs to be taken into account, for in an earlier study (Peters et al., 2001b) it was shown that the mean number of lamellae in sheaths from young monkeys is 5.6 and in old monkeys it is 7.0. As shown in Figure 8, when sheaths of these mean thicknesses for young and old monkeys are compared, the mean paranodal length for young monkeys is 1.81 μm and for old monkeys it is 2.07 μm. Consequently the mean paranodal length in old monkeys is, at most, only some 11% greater than in young monkeys.

This difference in the mean paranodal length is not sufficient to account for the 59% age-related increase in the frequency of paranodal profiles in layer 4 of area 17. Consequently, most of the age-related increase in frequency of paranodal profiles must be due to an increase in the number of internodes.

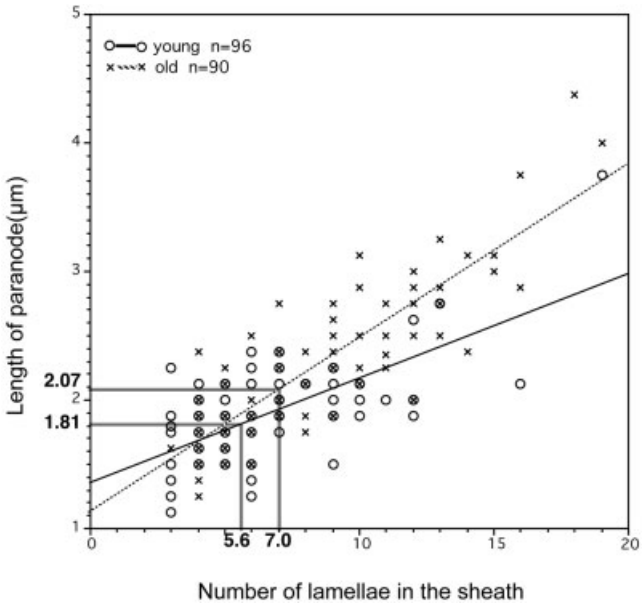

Fig. 8. A plot of the lengths of paranodes in area 17 of young and old monkeys vs. the number of lamellae in the internodal sheath. Imposed on the graphs are the mean thicknesses of sheaths in young (5.6 lamellae) and old (7.0 lamellae) monkeys. For sheaths of these thicknesses the mean length of the paranodes is 1.81 μm in young monkeys and 2.07 μm in old monkeys.

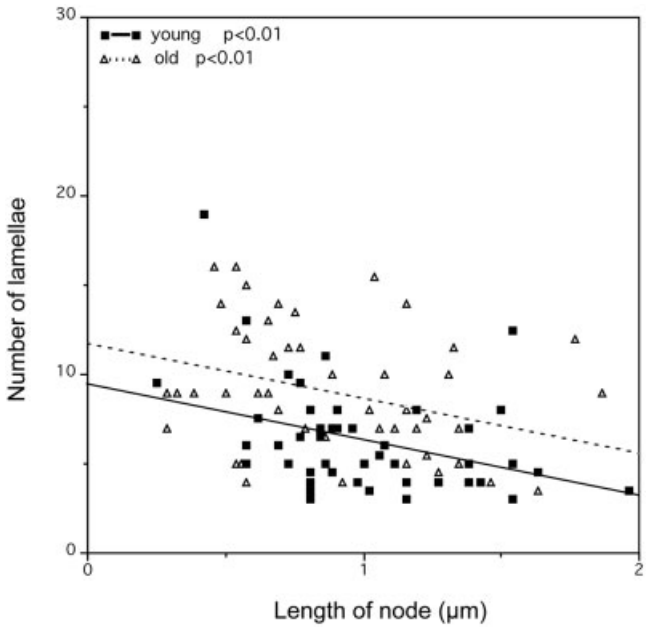

Fig. 9. Plots of the lengths of nodes of Ranvier in area 17 of young and old monkeys against the numbers of lamellae in the sheaths.

Lengths of nodes of Ranvier

Measurements were also made of the lengths of nodes of Ranvier in the photographic negatives taken of longitudinal sections of nerve fibers. Because of the helical turning off of the lamellae, the extent of the bare axolemma can be different on the two sides of the profile of the node. Consequently, the length of the node was measured on both sides and the mean value taken.

There is wide variation in the lengths of nodes, even in fibers with the same numbers of lamellae in their sheaths (Fig. 9). The lengths of nodes vary from 0.25–2 μm, and in general the nodes are shorter in nerve fibers with thick sheaths than in those with thinner sheaths ($P < 0.01$). However, for sheaths with the same numbers of lamellae there is no significant difference in lengths of nodes between young and old monkeys.

Correlation between cognitive impairment and frequency of paranodes

Since the increased frequency of paranodes along a nerve fiber can be expected to slow down the rate of conduction along that nerve fiber, the correlation between the cognitive impairment indices (CII) and the percentage of paranodal profiles observed in areas 17 and 46 (Table 1) was examined. As shown in Figure 10, there is a significant correlation between the CII and the percentage of paranodal profiles for area 46 ($P < 0.01$) but not for area 17.

Incidental observations on nerve fibers

An interesting observation made while examining the bundles of closely packed nerve fibers in area 17 of old monkeys is that not only is the frequency of paranodal and nodal profiles greater than in younger monkeys, but in old monkeys it is common to observe several of these profiles in close proximity to each other (Fig. 11). This situation is rarely encountered in young monkeys. The possible significance of this observation will be considered later, when it is suggested that some remyelination is taking place in cerebral cortex.

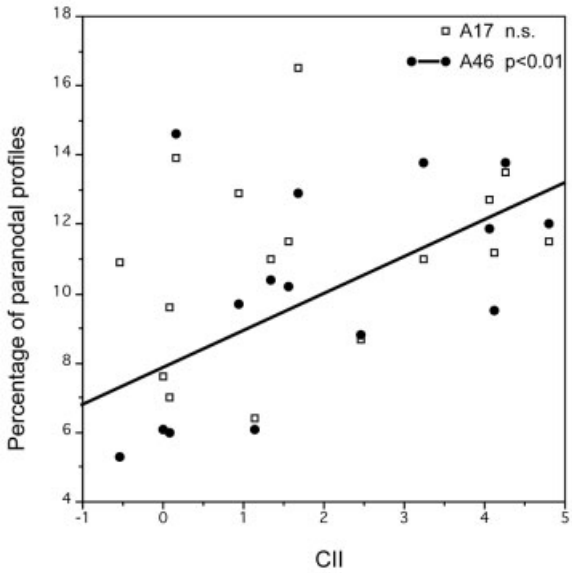

Fig. 10. A plot of the percentages of profiles that belong to paranodes in areas 17 and 46 of individual monkeys, against their cognitive impairment indices (CIIs). Increased CII values indicate increased cognitive impairment.

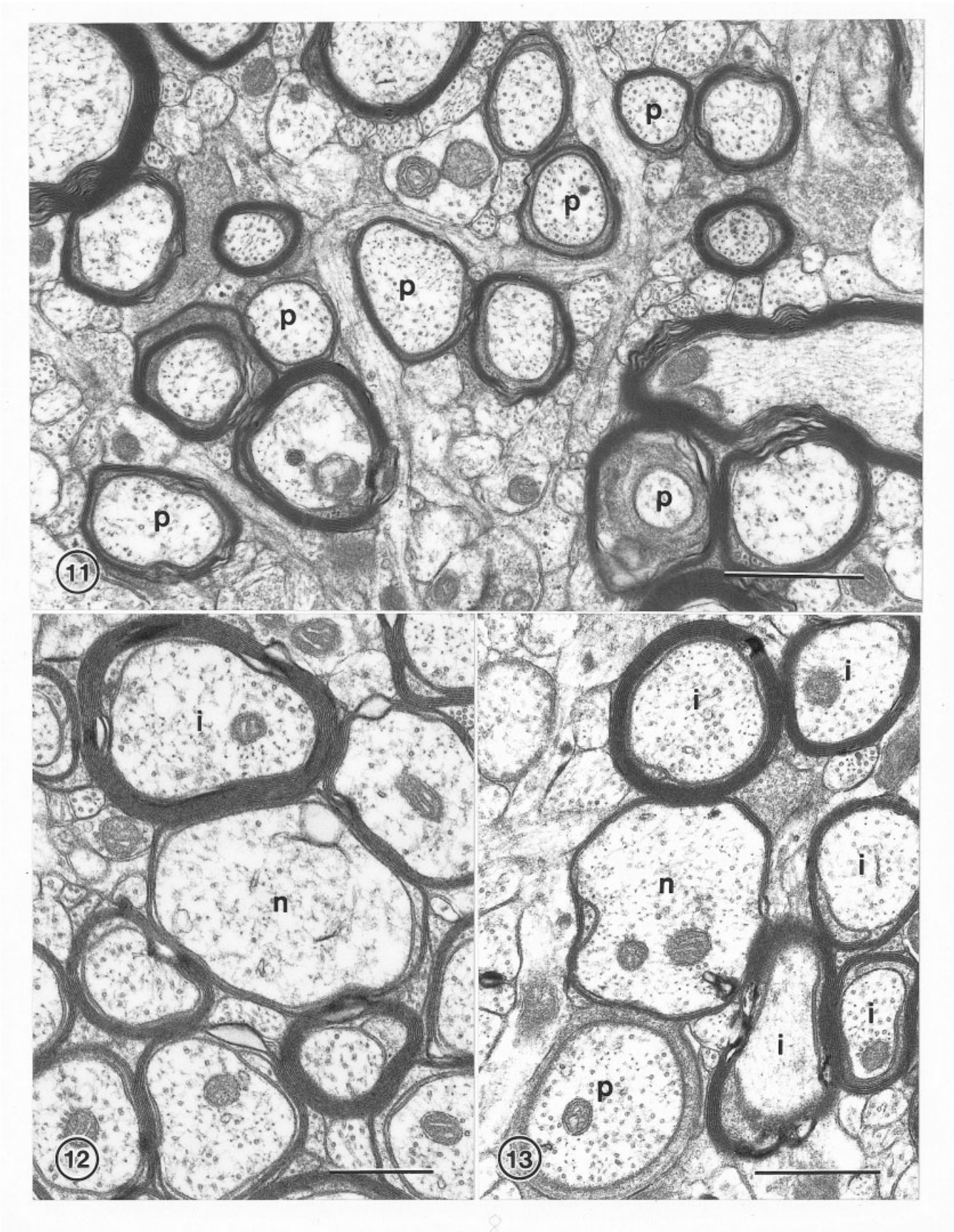

Figures 11–13

It is generally agreed that the signs revealing that remyelination is taking place are the occurrence of unusually thin myelin sheaths and of unusually short internodal lengths of myelin (e.g., Prineas and McDonald, 1997). Consequently, the nerve fibers in the vertical bundles in area 17 of old monkeys were examined to ascertain if any nerve fibers showed these morphological features. Both of them were encountered.

Unusually thin myelin sheaths. In both young and old monkeys, but more commonly in old monkeys, profiles of internodes are encountered in which the myelin sheaths are abnormally thin. Two examples are shown in Figures 12 and 13. The axons in each of these nerve fibers are about 1 micron in diameter and each has only two lamellae. The majority of axons of this diameter have sheaths with 5–9 lamellae (Peters et al., 2001), as can be seen by comparing these thin sheaths with the sheaths of adjacent nerve fibers having axons of similar diameters. The thinness of these particular sheaths suggests that they are in the early stages of myelin sheath formation.

Short internodal lengths of myelin. Examining complete internodal lengths of myelin in thin sections is difficult: the gently undulating nature of nerve fibers usually makes it almost impossible to follow them for any great distance in sections cut parallel to their lengths. Nevertheless, after an intensive search some short internodal lengths of myelin were encountered. The shortest one, illustrated in Figure 14 is only 3 μm long and two lamellae thick. Another short internode, shown in Figure 15, is 6 μm long and is one or two lamellae thick.

It should be added that some unusually long nodes of Ranvier were also encountered, as well as long stretches of bare axons emerging from myelin sheaths. But it could not be determined if these were lengths of axon that had been demyelinated or axons that had emerged from their sheaths prior to forming terminals.

Demyelination and phagocytosis of myelin

If there is a breakdown of some myelin sheaths with age, leading to demyelination, it would be expected that bare lengths of nerve fibers would occur and that there would be evidence of phagocytosis of myelin by neuroglial cells. Unfortunately, for the reasons given above, and because of an abundance of unmyelinated axons intermixed with the vertically oriented nerve fibers in cerebral cortex, demyelinated nerve fibers could not be identified. However, there is evidence that some demyelination is occurring because astrocytes with phagocytosed myelin have been occasionally encountered in layer 4 of both area 17 and area 46. Two examples of astrocytes with lamellar inclusions having the characteristics of myelin are shown in Figures 16 and 17. In Figure 16 the astrocyte is from area 17 and it contains a lamellar inclusion as well other inclusions that have dark and light components. The astrocyte shown in Figure 17 is from area 46 and in addition to a typical inclusion body its cytoplasm contains four profiles that appear to be derived from myelin, since they have a periodic structure with major dense and intraperiod lines that match the spacing of such lines in normal myelin. No myelin figures have been encountered in other types of neuroglial cells.

Use of a myelin basic protein (MBP) antibody, with the binding sites revealed using an immunogold amplification procedure, showed the MBP antibody to be bound to myelin sheaths (inset, Fig. 18), with some light labeling over oligodendroglial cells. The silver amplified colloidal gold appears as electron-dense particles. In addition, as shown in Figure 18, inclusions in some astrocytes were labeled. This indicates that some myelin is phagocytosed by astrocytes and then broken down, with the breakdown products being incorporated into the inclusion bodies characteristic of astrocytes.

Despite a lengthy search, no convincing labeling was encountered over the inclusions in microglial cells, pericytes, or oligodendrocytes.

DISCUSSION

Consideration of data on paranodal profiles

In electron micrographs of transverse sections through the vertical nerve fiber bundles in both areas 46 and 17, there is a significant, age-related increase in the frequency of the profiles of the paranodal portions of myelin sheaths. In area 17 the increase in frequency of paranodal profiles is 57%, while in area 46 it is 90%.

In area 17 of both young and old monkeys there is a significant correlation between the thickness of sheaths and the lengths of paranodes and in the vast majority of sheaths, those with less than 10 lamellae, the lengths of the paranodes are only slightly longer in old monkeys than in young ones (Fig. 8). However, even considered in conjunction with the fact that the mean number of lamellae in the myelin sheaths is 5.6 in young monkeys and 7.0 in old monkeys (Peters et al., 2001b), this increase in lengths of paranodes would only account for an age-related increase of 11% in the frequency of paranodal profiles. Consequently, it has to be concluded that most of the increase in the frequency of paranodal profiles in old monkeys is the result of an increase in the number of myelin internodes with age. Logically, this could only occur if there is demyelination followed by remyelination, to produce some shorter internodes of myelin in older monkeys.

Evidence that myelin is degenerating

As discussed previously (Peters et al., 2000), the age-related increase in the occurrence of altered myelin

Fig. 11. A portion of a nerve fiber bundle from area 17 of a 29-year-old monkey, AM 26. This micrograph illustrates the fact that in old monkeys it is not uncommon to encounter profiles of paranodes (p) in groups. Paranodes are recognized by the presence of a junction between the axolemma and the membrane on the inside of the myelin sheath Scale bar = 1 μm.

Fig. 12. Nerve fibers from area 17 of a 25-year-old monkey, AM 100. In the middle of the field is a nerve fiber (n) that has an unusually thin myelin sheath, composed of only two lamellae. The axon has a diameter of about 1 μm and normally axons of this size have sheaths consisting of 5–9 lamellae, as shown by the adjacent nerve fiber (i), which has a sheath with 9 lamellae. Scale bar = 0.5 μm.

Fig. 13. Nerve fibers from area 17 of a 27-year-old monkey, AM 27. As in Figure 7, the nerve fiber (n) in the middle of the field has a diameter of about 1 μm, and yet it has a sheath composed on only two lamellae. This is much thinner than usual, as can be seen by comparing the thickness of the sheath with that of the surrounding nerve fibers sectioned through their internodes (i). Note the paranode (p) at the bottom of the field. Scale bar = 0.5 μm.

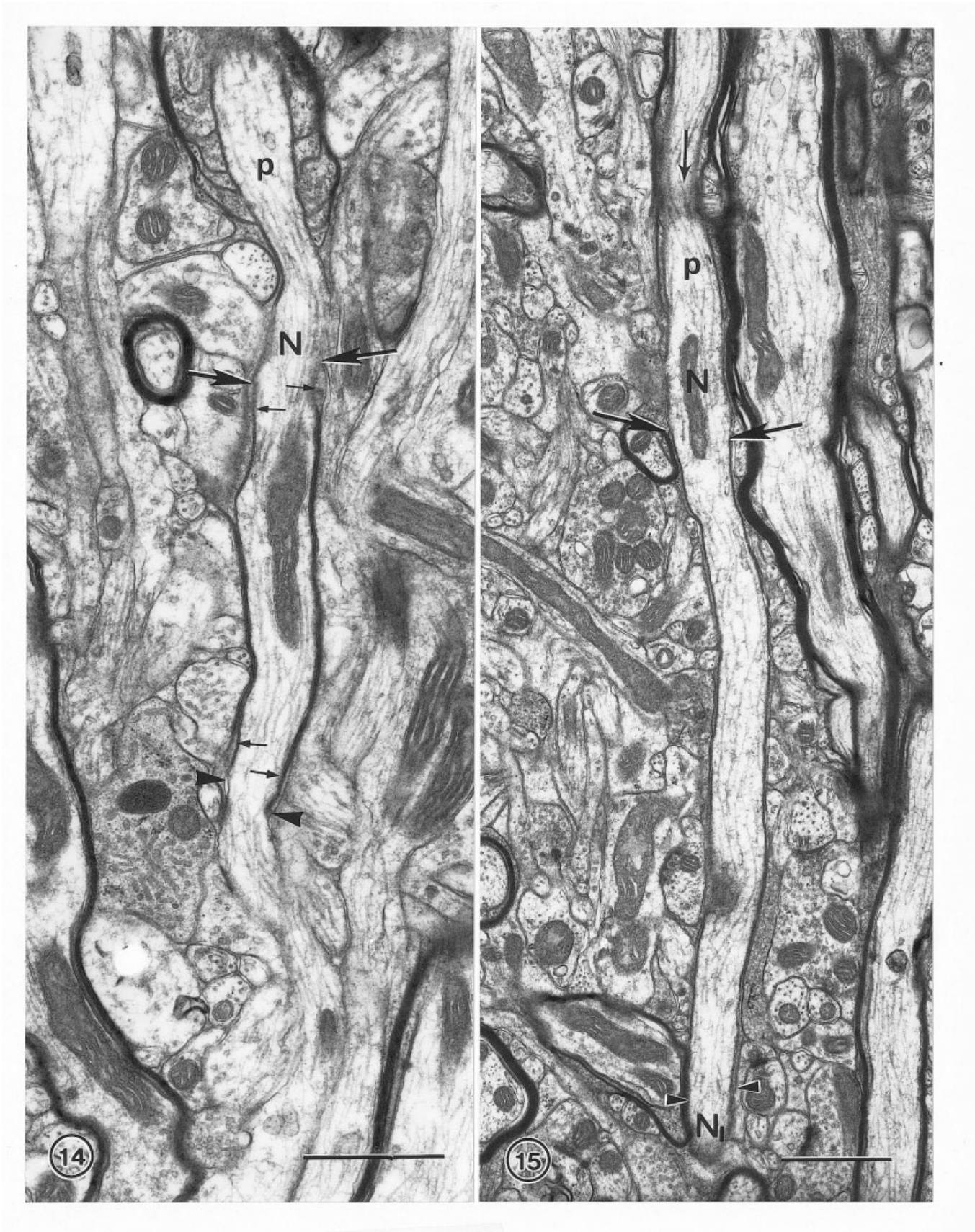

Figures 14 and 15

sheaths, and in particular ones that have pockets of dense oligodendrocytic cytoplasm or splitting of the sheath, suggests that myelin sheaths are breaking down with age. That these are signs of degeneration of myelin is suggested by the occurrence of similar alterations during early phases of demyelination in a number of situations. For example, in cuprizone poisoning dark cytoplasm occurs in the inner tongue processes of myelin sheaths and other sheaths show splitting of the intraperiod line to form balloons (Ludwin, 1978, 1995). Dark cytoplasm is also present in the degenerating myelin of mice with a myelin-associated glycoprotein deficiency (Lassman et al., 1997). Myelin balloons have been described as a consequence of spontaneous degeneration in the gerbil cochlear nucleus (Faddis and McGinn, 1997) and they also occur in the early phases of Wallerian degeneration (Franson and Ronnevi, 1989); in severe diabetes (Tamura and Parry, 1994); in experimental toxicity produced by triethyl tin (Hirano, 1989); and as a result of copper poisoning (Hull et al., 1974). They also occur as a result of late-onset degeneration in genetically engineered mice with an increased dosage of the proteolipid protein gene (Anderson et al., 1998) and in mice that are lacking the galactolipid galactocerebroside (Coetzee et al., 1996, 1998). Thus, it can be concluded that the age-related alterations in myelin are indications that sheaths are breaking down. Moreover, the age-related alterations largely affect the myelin and only rarely is the axon involved.

Phagocytosis of myelin

We have encountered no morphological signs that extensive demyelination, such as myelin stripping by microglial cells, is taking place, but there may be several reasons for this. One reason is that in cerebral cortex it is myelin that is mainly affected by aging, and not the nerve fiber as a whole. We have encountered some degenerating axons in cortex, but they are few in number and in striate cortex they do not lead to significant reduction in the numbers of nerve fibers (Peters et al., 2000; Nielsen and Peters, 2000). Stimulation of microglial cells seems to be only obvious in conditions in which there is Wallerian degeneration (see Kreutzberg et al., 1997), or in conditions in which there is an extensive loss of nerve fibers, as we have encountered in the optic nerves of old monkeys (Sandell and Peters, 1999, 2002).

Some of the microglial cells in the aging cerebral cortex do contain phagocytosed debris, but none of the phagocytosed material in these cells has the appearance of myelin. However, myelin figures have been encountered in some astrocytes (see Figs. 16, 17) and some of the more amorphous inclusions in astrocytes label with antibodies to myelin basic protein (Fig. 18). Since none of the inclusions in either microglial cells or oligodendrocytes of old monkeys labeled with this antibody, it appears that in the cerebral cortex of old monkeys the astrocytes are responsible for phagocytosing the degenerating myelin (also see Peters and Sethares, 2002).

A second reason for lack of activation of microglia could be that only a few internodal segments of myelin in cerebral cortex are degenerating simultaneously. Such low levels of degeneration would occur if only a few oligodendrocytes were affected at any one point in time and the sheaths belonging to them broke down, producing segmental demyelination, in which only a few short lengths of neighboring axons bare.

Remyelination

Such segmental demyelination, followed by remyelination, would lead to an increase in the numbers of internodal lengths of myelin and produce the increased frequency of paranodal profiles encountered in old monkeys. In situations in which remyelination occurs, in either experimental or naturally occurring demyelinating states, the remyelinating axons display internodes that are inappropriately short for the diameter of the axon and sheaths that are inappropriately thin (e.g., Gledhill and McDonald, 1977; Hirano, 1989; Kreutzberg et al., 1997; Ludwin, 1978, 1995; Prineas and McDonald, 1997). Short internodal lengths of myelin also occur during development, when myelin is first being laid down, and in the spinal cord and corpus callosum of the cat, Remahl and Hildebrand (1990) found the majority of early, uncompacted sheaths to be about 10 μm long, although they encountered some that were as long as 150 μm. Nerve fibers with inappropriately thin myelin sheaths do occur in the cortices of old monkeys (see Figs. 12, 13) and we have also ascertained that short internodal lengths of myelin exist (Figs. 14, 15). It seems unlikely that these entities would not exist unless remyelination is occurring during aging.

Correlation with cognition

In both area 17 and in area 46, the increased frequency of paranodal profiles correlates with increasing age, but it is only in area 46 that the frequency of paranodal profiles correlates with cognitive decline. However, in both area 17 (Peters et al., 2000) and in area 46 (Peters and Sethares, 2002) there is a significant correlation between the age-related alterations of myelin and the CII. It is suggested that these correlations between the breakdown of myelin and the increase in cognitive deficits occur because the breakdown of myelin leads to changes in conduction rates along myelinated nerve fibers, resulting in a loss of synchrony in cortical circuits. Of course, increasing the number of internodal lengths of myelin will also affect the rate of conduction. The reason why there is only a correlation between paranodal profile frequency and CII for area 46, and not for area 17, may be because prefrontal cortex has a greater role than area 17 in subserving cognition. In this respect it is also of interest that in the aging cerebral cortex there is a decrease in the thickness of layer 1 and a loss of synapses, but again these changes only correlate with the CII in area 46 (Peters et al., 1998) and not in area 17 (Peters et al., 2001a).

Fig. 14. A longitudinally sectioned nerve fiber in layer 4 of area 17 in a 25-year-old monkey, AM 100. At the top of the field is a paranode (p) and just below it is a node of Ranvier (N). The undercoating of the axolemma is visible on the left side of the node. The axon then enters into a thin sheath (large arrows) that is two lamellae thick and 3 μm long. The other end of this short internode is indicated by the arrowheads. At both ends of the short internode pockets of paranodal cytoplasm are visible (small arrows). Scale bar = 1 μm.

Fig. 15. A longitudinally sectioned nerve fiber in layer 4 of area 17 from a 25-year-old monkey, AM 100. At the top of the field the axon emerges from a paranode (p), where the transverse bands are visible (small arrow). Below the paranode is a node of Ranvier (N), where the axon has a dense undercoating. The axon then enters a sheath (large arrows) that is one or two lamellae thick. This thin sheath extends for 6 μm and terminates (arrowheads) at an obliquely sectioned node of Ranvier (N_1), which can be identified by the axolemmal undercoating. Scale bar = 1 μm.

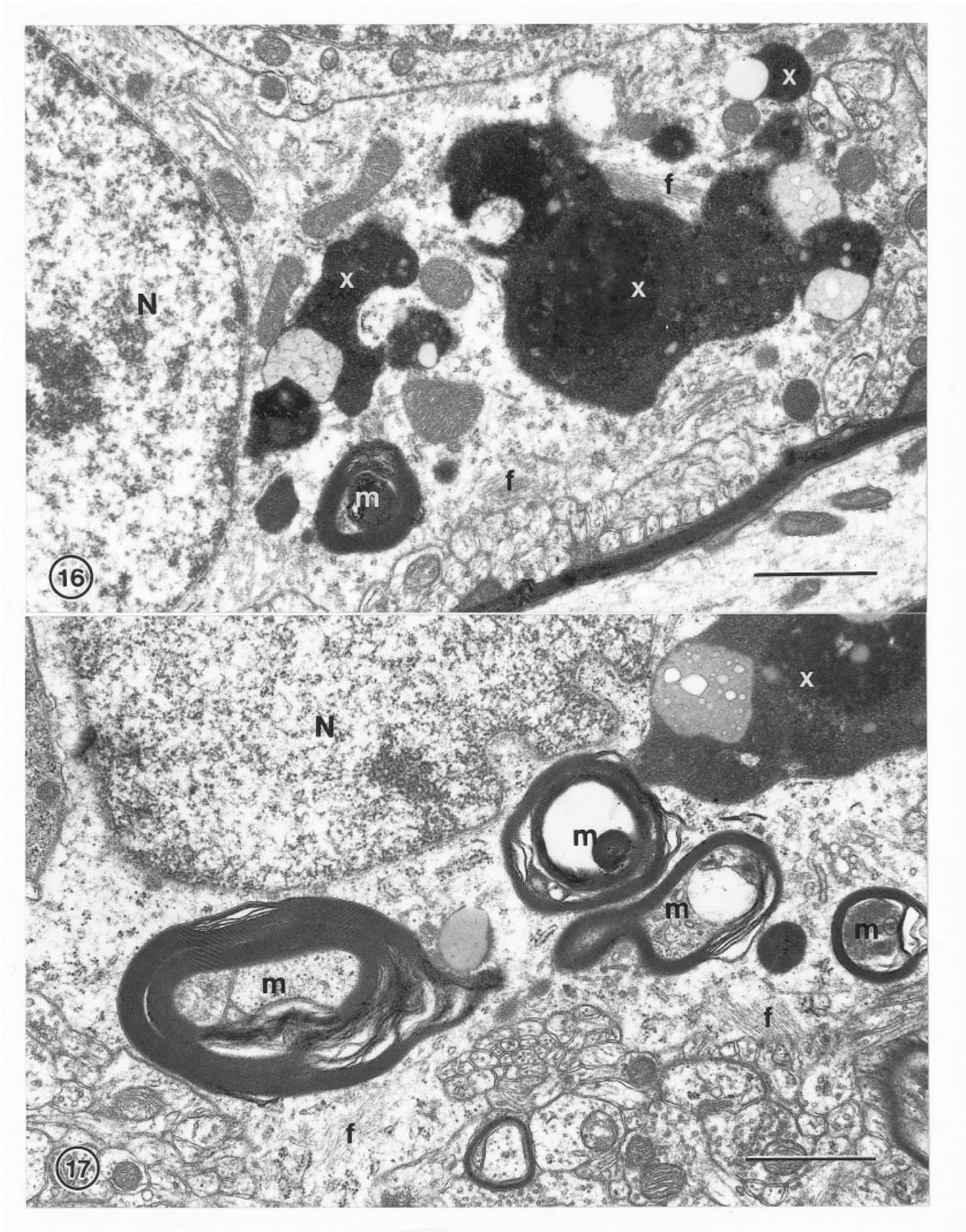

Figures 16 and 17

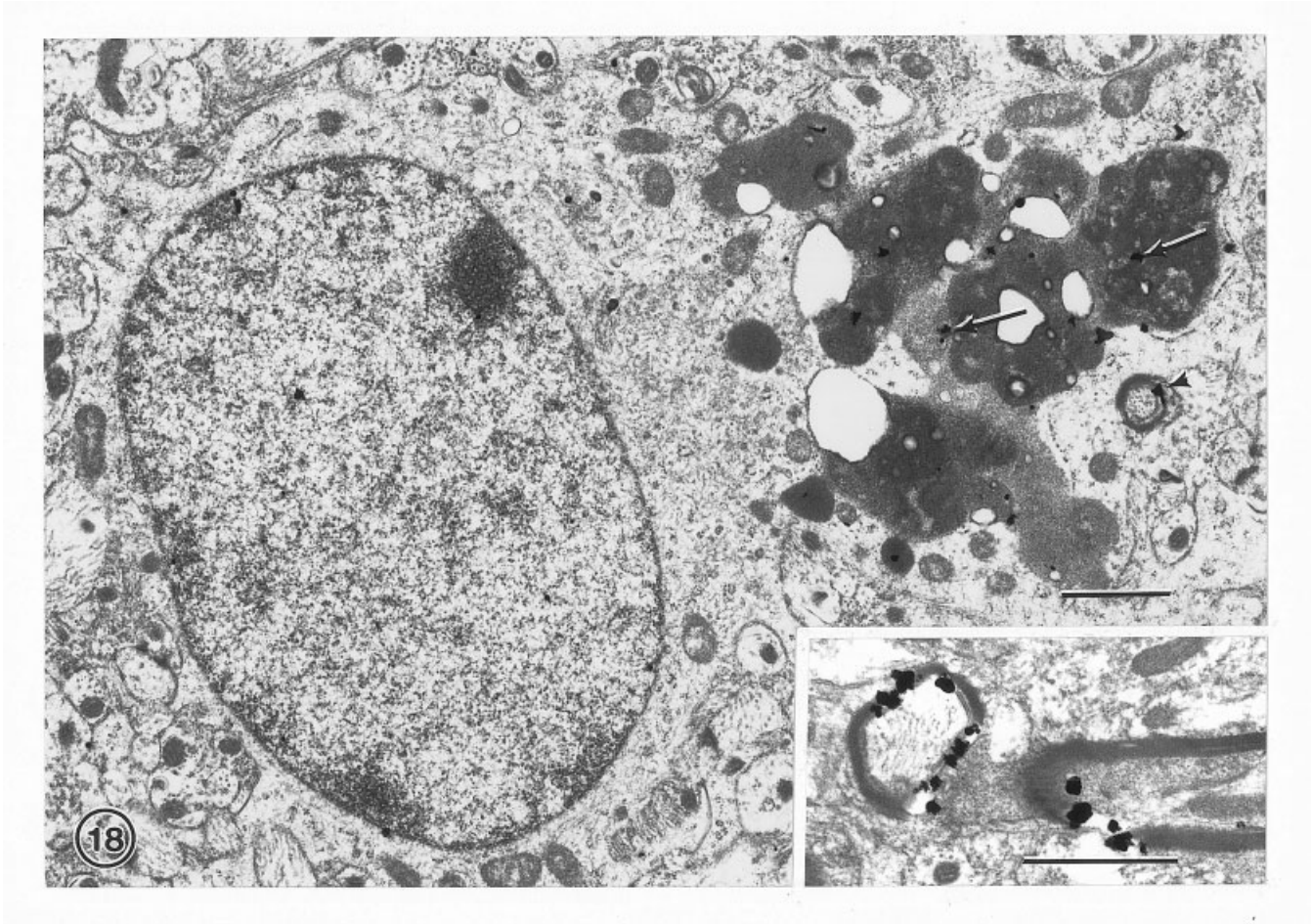

Fig. 18. An astrocyte from layer 4 of primary visual cortex in a 25-year-old monkey, AM 100. The inclusion body in the astrocyte has bound antibody to myelin basic protein, as indicated by the concentration of silver-amplified particles of colloidal gold overlying the inclusion (arrows). A nearby small myelin sheath also has a gold particle over it (arrowhead). There are three or four particles over the cytoplasm and nucleus of the astrocyte, but they are not in the same concentration as the particles over the inclusion body. The inset shows myelin sheaths that are labeled with the antibody. Scale bars = 1 μm.

A hypothesis

From the data generated in this study it is suggested that during normal aging in the cerebral cortex some oligodendroglial cells become unable to sustain their myelin sheaths. This would result in their internodal lengths of myelin breaking down and degenerating, as indicated by the presence of dense, degenerating oligodendroglial cytoplasm within some sheaths and by the formation of myelin balloons. However, we have no direct evidence that internodal lengths of myelin are lost. But evidence that some myelin is degenerating comes from the existence of phagocytosed inclusions with the structural characteristics of myelin in some astrocytes and from the fact that some of the amorphous inclusion bodies in astrocytes label with antibodies to myelin basic protein.

It is suggested that after the internodal lengths of myelin belonging to the affected oligodendrocytes have degenerated, remyelination takes place, with the original internodal lengths of myelin being replaced by new, shorter lengths of myelin. As a consequence, there is an increase in the frequency of profiles of paranodes. Because of these interrelated events there is a significant correlation between the frequency of paranodal profiles and both age and the frequency of occurrence of profiles of altered sheaths. The concept that there is remyelination is also supported by the demonstration that some short internodal lengths of myelin occur in striate cortex of old monkeys and that some nerve fibers have inappropriately thin

Fig. 16. Part of an astrocyte in area 17 of a 32-year-old monkey, AM 41. A portion of the nucleus (N) is present on the left and the cytoplasm of the astrocyte contains bundles of filaments (f) as well as a number of age-related inclusions (x). Another inclusion (m) consists of phagocytosed myelin, in which the lamellae are still visible. Scale bar = 1 μm.

Fig. 17. Part of an astrocyte in area 46 of a 25-year-old monkey, AM 100. A portion of the nucleus (N) is seen in the upper half of the picture and the cytoplasm contains the characteristic filaments (f). The cytoplasm also contains an inclusion body (x) as well as four lamellar bodies that are obviously derived from myelin (m). The cytoplasm inside the phagocytosed myelin has the characteristics of astrocytic cytoplasm. Scale bar = 1 μm.

sheaths. Both of these features are considered to be the hallmarks of remyelination.

It was also observed that in transverse sections of bundles of nerve fibers in striate cortex of old monkeys it is not uncommon to encounter profiles of paranodes in groups. It is suggested that these groups originate as follows. If the bare lengths of axons that are being remyelinated were originally ensheathed by myelin derived from the same oligodendrocyte, the bare lengths can be expected to be in proximity to each other. Consequently, when new oligodendrocytes remyelinate these bare lengths of axons by forming shorter internodes, it is likely that paranodes belonging to the new short internodes will be in a similar transverse plane. The result would be that in cross sections of nerve fiber bundles some profiles of paranodes occur in groups.

The increase in the number of internodal lengths of myelin with age presumably requires an increase in the population of oligodendrocytes. Such an increase in the numbers of oligodendrocytes was indicated in our earlier study of neuroglial frequency in the aging monkey striate cortex (Peters et al., 1991a), and an increase in the numbers of oligodendrocytes is suggested by the fact that, with age, groups and rows of oligodendrocytes become increasingly common in this same cortex (Peters, 1996). How the population of oligodendrocytes in cerebral cortex changes with age will be investigated more fully in the next phase of this study. It will also be determined if oligodendroglial progenitor cells are present in the cortices of mature monkeys, since it is likely that such cells, and not mature oligodendrocytes, are the source of new oligodendrocytes (e.g., Norton, 1966; Nishiyama et al., 1999; Levine et al., 2001).

LITERATURE CITED

Anderson TJ, Schneider A, Barrie JA, Klugmann M, McCulloch MC, Kirkham D, Kyriakides E, Nave K-A, Griffiths IR. 1998. Late-onset degeneration in mice with increased dosage of the proteolipid protein gene. J Comp Neurol 394:506–519.

Bennett V, Lambert S. 1999. Physiological roles of axonal ankyrins in survival of premyelinated axons and localization of voltage-gated sodium channels. J Neurocytol 28:303–318.

Bhat MA, Rios JC, Lu Y, Garcia-Fresco GP, Ching W, St Martin M, Li J, Einheber S, Chesler M, Rosenbluth J, Salzer JL, Bellen HJ. 2001. Axon-glia interactions and the domain organization of myelinated axons requires neurexin IV/caspar/paranodin. Neuron 30:369–383.

Brodmann K. 1905. Beitrage zur histologischen Lokalization der Grosshirnrinde. IIIte Mittlung: Die Rindfelder der niederen Affen. J Psychol Neurol 4:177–226.

Coetzee T, Fujita N, Dupree J, Shi R, Blight A, Susuki K, Popko B. 1996. Myelination in the absence of galactocerebroside and sulfatide: normal structure with abnormal function and regional instability. Cell 86:209–219.

Coetzee T, Susuki K, Popko B. 1998. New perspectives of the function of myelin galactolipids. Trends Neurosci 21:126–130.

Faddis BT, McGinn MD. 1997. Spongiform degeneration of the gerbil cochlear nucleus: an ultrastructural and immunohistochemical evaluation. J Neurocytol 26:625–635.

Feldman MF, Peters A. 1998. Ballooning of myelin sheaths in normally aged macaques. J Neurocytol 27:605–614.

Franson P, Ronnevi L-O. 1989. Myelin breakdown in the posterior funiculus of the kitten after doral rhizotomy: a qualitative and quantitative light and electron microscopic study. Neurosci Lett 195:93–96.

Gledhill RF, McDonald WI. 1977. Morphological characteristics of central demyelination and remyelination: a single fiber study. Ann Neurol 1:552–560.

Herndon J, Moss MB, Killiany RJ, Rosene DL. 1997. Patterns of cognitive decline in early, advanced and oldest of the old aged rhesus monkey. Behav Res 87:25–34.

Hirano A. 1989. Review of the morphological aspects of remyelination. Dev Neurosci 11:112–117.

Hull JM, Blakemore W. 1974. Chronic copper poisoning and changes in the central nervous system of sheep. Acta Neuropathol 29:9–24.

Killiany RJ, Moss MB, Rosene DL, Herndon J. 2000. Recognition memory function in early senescent rhesus monkeys. Psychobiology 28:45–56.

Kreutzberg G, Blakemore WF, Graeber MB. 1997. Cellular pathology of the central nervous system. In: Graham DI, Lantos PL, editors. Greenfield's neuropathology, 6th ed. London: Arnold. p 85–156.

Lassman H, Bartsch U, Montag D, Schachner M. 1997. Dying-back oligodendrogliopathy: a late sequel of myelin-associated glycoprotein deficiency. Glia 19:104–110.

Levine JM, Reynolds R, Fawcett JW. 2001. The oligodendrocyte precursor cell in health and disease. Trends Neurosci 24:39–47.

Ludwin SK. 1978. Central nervous system demyelination and remyelination in the mouse: an ultrastructural study of cuprizone toxicity. Lab Invest 39:597–612.

Ludwin SK. 1995. Pathology of the myelin sheath. In: Waxman SG, Kocsis JD, Stys PK, editors. The axon: structure, function and pathophysiology. New York: Oxford University Press. p 412–437.

Nielsen K, Peters A. 2000. The effects of aging on the frequency of nerve fibers in rhesus monkey striate cortex. Neurobiol Aging 21:621–628.

Nishiyama A, Chang A, Trapp BD. 1999. NG2+ glial cells: a novel glial cell population in the adult brain. J Neuropathol Exp Neurol 58:1113–1124.

Norton WT. 1996. Do oligodendrocytes divide? Neurochem Res 21:495–503.

Peters A. 1966. The node of Ranvier in the central nervous system. Q J Exp Physiol 51:229–236.

Peters A. 1996. Age-related changes in oligodendrocytes in monkey cerebral cortex. J Comp Neurol 371:153–163.

Peters A, Sethares C. 1996. Myelinated axons and the pyramidal cell modules in monkey primary visual cortex. J Comp Neurol 306:1–23.

Peters A, Sethares C. 2002. Aging and the myelinated fibers in prefrontal cortex and corpus callosum of the monkey. J Comp Neurol 442:277-291.

Peters A, Josephson K, Vincent SL. 1991a. Effects of aging on the neuroglial cells and pericytes within area 17 of the rhesus monkey cerebral cortex. J Comp Neurol 229:384–398.

Peters A, Palay SL, Webster DeFH. 1991b. The fine structure of the nervous system: neurons and their supporting cells. New York: Oxford University Press.

Peters A, Leahu D, Moss MB, McNally KJ. 1994. The effects of aging on area 46 of the frontal cortex of the rhesus monkey. Cereb Cortex 6:621–635.

Peters A, Sethares C, Moss MB. 1998. The effects of aging on layer 1 in area 46 of prefrontal cortex in the rhesus monkey. Cereb Cortex 8:671–684.

Peters A, Moss MB, Sethares C. 2000. Effects of aging on myelinated nerve fibers in monkey primary visual cortex. J Comp Neurol 419:364–376.

Peters A, Moss MB, Sethares C. 2001a. The effects of aging on layer 1 of primary visual cortex in the rhesus monkey. Cereb Cortex 11:93–103.

Peters A, Sethares C, Killiany RJ. 2001b. Effects of age on the thickness of myelin sheaths in monkey primary visual cortex. J Comp Neurol 435: 241–246.

Prineas JW, McDonald WI. 1997. Demyelinating diseases. In: Graham DI, Lantos PL, editors. Greenfield's neuropathology, 6th ed. London: Arnold. p 813–896.

Raine CS. 1984. Morphology of myelin and myelination. In: Morell P, editor. Myelin. New York: Plenum Press. p 1–50.

Remahl S, Hildebrand C. 1990. Relation between axons and oligodendroglial cells during initial myelination. II. The individual axon. J Neurocytol 19:883–898.

Rosenbluth J. 1995. Glial membranes and axoglial junctions. In: Waxman SG, Koscis JD, Stys PK, editors. The axon: structure, function and pathophysiology. New York: Oxford University Press. p 613–633.

Sandell JH, Peters A. 1999. The effects of age on nerve fibers in the rhesus monkey optic nerve. J Comp Neurol 429:541–553.

Sandell JH, Peters A. 2002. Effects of age the glial cells in the rhesus monkey optic nerve. J Comp Neurol 445:13–28.

Sturrock RR. 1976. Changes in neuroglia and myelination in the white matter of aging mice. J Gerontol 31:513–522.

Tamura E, Parry GJ. 1994. Severe radicular pathology in rats with long standing diabetes. J Neurol Sci 127:29–35.

Walker AE. 1940. A cytoarchitectural study of the prefrontal area of the macaque monkey. J Comp Neurol 73:59–86.